7th International Conference on the Durability of Concrete Structures
20-22 May 2022
University of Jinan, Jinan, Shandong, China

Carbonation resistance enhancement of cement mortars with recycled plastics using ethylene-vinyl acetate and nanosilica

Ahmed Al-Mansour, Rijiao Yang, Chengji Xu, Shan Chen, Yu Peng, Qiang Zeng*
College of Civil Engineering and Architecture, Zhejiang University, Hangzhou, 310058, PR China
* Corresponding author: cengq14@zju.edu.cn (Q. Zeng)

ABSTRACT

Plastic has surpassed most of the man-made materials, and it has been accumulated as “waste” in the environment for several decades. Replacement of natural aggregates in concrete with recycled waste plastic (RWP) attracted great attentions in recent years due to the high potentials of recycling waste plastic. This employment of RWPs in concrete, however, was accompanied by reduction in mechanical properties and durability performances (e.g., carbonation) due to the poor interactions between RWP and cement matrix. The aim of this study is to lessen the mechanical defects of cement mortars with RWPs and enhance the carbonation resistance by employing Ethylene-vinyl acetate (EVA) and nanosilica (nS) in the mortar mixtures. 2 to 4 % of EVA and nS were substituted for cement in mortars with 10 and 15 % RWPs. Strength and carbonation resistance of the mortars were measured. Microstructure was investigated by scanning electron microscopy (SEM) and energy-dispersive X-ray spectroscopy (EDS). Results showed that as much as 5.5 % improvement in strength and 50% reduction in carbonation depth were recorded for mortars with the EVA-nS addition. EVA created polymer films around the RWPs to improve cohesion with the cement matrix, while nS filled the pores and enhanced the material compactness. Our findings would pave a path to fabricate stronger and more durable cement mortar with RWP.

1. INTRODUCTION

Carbonation of concrete has been considered a major degradation factor in warm and humid climates that may raise the risks of steel bar corrosion [1]. The reaction starts at the exposed surface of a concrete member (or called covercrete) that functions as a shield protecting reinforcing rebars [2, 3]. In concrete, the calcium-rich phases, such as calcium silicate hydrate (CSH) and calcium hydroxide ($Ca(OH)_2$) can react with carbon dioxide (CO_2) producing calcium carbonate and water.

The formation of highly stable calcium carbonate may enhance mechanical properties and reduce permeability of concrete [4, 5]. In this regime, accelerated carbonation has been used to enhance shrinkage and mechanical properties of recycled aggregates [6-9]. However, the neutralization of highly alkaline concrete due to carbonation reactions can cause drastic decreases of pH from12-14 down to 8-9, which in turn leads to depassivation of rebars. In other words, in carbonated concrete, reinforcing rebars corrodes easily as if they were in contact with water [10].

Compared with the carbonation reactions that almost take place instantaneously, the penetration of CO_2 into covercrete may take tens or even thousands of years to get to the reinforcement depending on several factors, e.g., permeability and thickness of the covercrete, and concentration of harmful species in the environment. Therefore, the penetration rate of CO_2 from the atmosphere into concrete may be a decisive process for the occurrence of carbonation. Generally, carbonation depth, a most widely used engineering index of carbonation rate in concrete, is proportional to the square root of time. Different mathematical models were developed to predict carbonation rate and depth based on certain relevant parameters of cement pasts and environments [11, 12].

Meanwhile, the massive natural resources and energy consumption for the manufacture of concrete aggregates has also gained increasing attention. Annual production of plastic wastes arrived at 120 kg/capita [13], and at present, recycling waste plastics to partially replace natural aggregate would show high potentials to reduce massive plastic wastes owing to the large scale yearly production of concrete (30 billion ton [14]). Use of recycled waste plastic (RWP) in concrete offer preferable properties such as weight reduction and higher impact load resistance [15, 16]. However, degradation of mechanical properties of concrete when natural aggregates are partially replaced by RWPs has always limited such implementation [17, 18], which is mainly attributed to the inferior compatibility of plastic aggregates and cement matrix. For example, 60% reduction in compressive strength was recorded when 50% of sand was replaced by recycled low-density polyethylene (LDPE) plastic [19]. To

compensate such degradation and enhance compatibility between plastic aggregates and cement matrix, several additives have been proposed, such as ethylene-vinyl acetate copolymer (EVA) [15, 20], nanosilica (nS) [21, 22], fly ash (FA) [23], and granular blast-furnace slag (GBFS) [24].

Physically, CO_2 molecules can migrate into concrete through the open channels, therefore, reduction in open porosity is a promising way to increase carbonation resistance. In this regime, supplementary cementitious materials have been applied to partially replace cement to obtain improved characteristics, such as strengths and toughness, in addition to carbonation resistance [25-28]. Alternatively, use of polymers (e.g., EVA, a copolymer of vinyl acetate and ethylene) in concrete to tune the matrix microstructure may create a more porous but less permeable structure [29]. In addition, EVA particles can form multi-later coatings around big particles, enhancing adhesion and crack resistance [30, 31]. However, the porous microstructure of polymer-altered cement matrix lowers the strength of cementitious materials [25, 29, 30]. Therefore, great incentives rise to mitigate the strength reduction of concrete with RWP and EVA. Nanomaterials, such as nanosilica (nS), have also been proved to improve compactness, strengths, and stability of concrete in aggressive environments [32]. Substantial reduction in carbonation of cement pastes with nS was reported [33].

Inspired by the aforementioned material improvement with EVA and nS, this study aims to develop RWP cement mortars that have enhanced strength and carbonation resistance. The data includes physical and mechanical benefits of the materials used (RWPs, EVA, and nS), in addition to macro and micro insights of cement matrices due to carbonation. Scanning electron microscopy (SEM) and energy-dispersive X-ray spectroscopy (EDS) were used to observe microstructural changes. The findings of this study provide a preliminary guidance towards the fabrication of durable and sustainable concrete.

2. Materials and methods

2.1. Materials and specimens

A Chinese PI 42.5 Portland cement (equivalent to ASTM type 1) was used as the binder. The standard consistency and specific surface area of the cement are 24.8% and 355 m^2/kg, respectively. Main minerals of the clinkers include: 59.03% C_3S, 16.47% C_2S, 6.79% C_3A, and 11.73% C_4AF.

The sand used as fine aggregates for all specimens meets the Chinese standards GSB 08-1337-2018. The maximum particle size of the sand is less than 4 mm. A recycled polypropylene (PP) obtained from Xiamen Keyuan Plastic Co., Ltd., was adopted to partially replaced sand with PP. The maximum particle size of the RWP was 2.18 mm. The original applications of this PP plastic include packaging, furnishings, toys, food and water containers, etc.

Redispersible EVA and nS were purchased from Aladdin Chemical Co., Ltd. Both EVA and nS had spherical particles with average sizes of 271±29 mm and 91±8 mm, respectively. The specific particle size parameters of EVA and nS were obtained by NANOSIGHT NS500 machine (Malvern Instruments Ltd) and are provided in Table 1. An alkaline solution (2 wt% sodium hydroxide) was first mixed with both inorganic and organic nano particles to achieve a better dispersion before they were mixed with other components of cement mortars.

Table 1. Main physical properties of nanosilica (nS) and ethylene-vinyl acetate (EVA).

	nS	EVA
Density (g/cm^3)	2.4	1.3
Mean particle size (nm)	91 ± 8	571 ± 29
D10 (nm)	78 ± 10	110 ± 18
D50 (nm)	181 ± 25	377 ± 33
D90 (nm)	223 ± 40	663 ± 80

The replacement ratios of sand by PP were selected as 10% and 15%, and the total contents of EVA and nS were limited to 4% by cement weight. Table 2 lists the mortar mix proportions in kg for 1 m^3, where P, E and N stand for plastic, EVA, and nS, respectively, and the number besides each letter represents the content of each additive. Water-to-cement (w/c) ratio was slightly adjusted for each mixture to get a consistent slump of 115±10 mm.

EVA nano particles were firstly mixed in the 2 wt% sodium hydroxide solution for 5 min at 400 rpm. During that, nS was gradually added to obtain a milky organic-inorganic suspension without obvious agglomeration. After that, RWP was mixed with this suspension at 400 rpm for another 5 min. Simultaneously, cement and sand were dry-mixed, and then the prepared solution was poured in the homogenous cement-sand mixture. Another stirrings at 60 rpm for 2 min were performed to attain the cement mortar slurries. Finally, the well mixed mortar slurries were cast in cubic (5 x 5 x 5 cm^3) and prismatic molds (4 x 4 x 16 cm^3) with vibrations for 30 s. Instantly, a thin layer of plastic film was used to cover the top surface of mortar specimens to avoid water evaporation. After a primary curing for 24 h, specimens were demolded and stored in a curing room with a temperature of 22±3 ^oC and relative humidity of 98±2% until testing ages.

Table 2. Designed mortar mixtures.

Mix ID	Mortar mix proportions in kg/m^3						EVA/ cement (%)	nS/ cement (%)
	Cement content	EVA content	nS content	Fine aggregate	Plastic	Water		
P10	525	0.0	0.0	1245	149	236	0	0
P10E2N1*	506	10.5	5.3	1245	149	240	2	1
P10E2N2	496	10.5	10.5	1245	149	242	2	2
P15	525	0.0	0.0	1155	224	236	0	0
P15E2N1	506	10.5	5.3	1155	224	240	2	1
P15E2N2	496	10.5	10.5	1155	224	242	2	2

* P: polypropylene, E: EVA, N: nanosilica.

2.2. Tests

Compressive and flexural strengths were conducted using INSTRON 8802 in force control at 75 kN/min and displacement control at 1 mm/min, respectively. 18 cubes were tested for compression, and 18 prisms for flexure.

Carbonation tests were conducted using the prismatic specimens. An oven-drying at 50 ^oC for 24 h was performed to all spcimens to remove the capillary water. This dyring scheme would facilitate the carbonation of mortars. After drying, five faces of each specimen were sealed with paraffin to allow a one-dimension carbonation. Once the paraffin hardened, specimens were carefully placed into a carbonation chamber at 80±5% humidity, 30±3 ^oC temperature, and 20±2% CO_2 concentration for 21 d [34]. Later, the mortar prisms were split and sprayed with 1% phenolphthalein alcohol solution. Phenolphthalein is a colorless acid indicator, which turns purple-red when it meets a high alkalinity (pH > 9.5) [35]. So, generally the uncarbonated cement matrix shows purple-red, while the carbonated one doesn't show color changes. The specific steps for carbonation tests are shown in Figure 1. Five measurements at different locations from the uncoated edge to the purple-ish zone were averaged to obtain the carbonation depth (X_{av}); see Figure 2.

Microstructural observation was conducted by FEI Quanta 650 FEG scanning electron microscopy (SEM) with its energy-dispersed X-ray spectroscopy (EDS) system. Small mortar pieces were collected from the outer surface of the damaged prisms for the SEM/EDS tests. During the microstructure tests, the accelerating voltage was set at 20 keV.

3. Results and discussion

3.1. Strengths

Figure 3 shows the compressive strength and relative changes of the mortars with RWP. The increase of RWP content in the mortars from 10% to 15% caused the reduction in compressive strength by about 12% independent of uses of EVA and nS. The reductions in compressive strength may be due to the weak body of plastic itself and the inferior cohesion with cement paste among other natural aggregates [17, 36].

Figure 1. Schemes of carbonation test: oven drying, paraffin surface sealing, carbonation for 21 d, and phenolphthalein test.

Mortars with EVA and nS showed increased compressive strength. An average increase of 3.8% and 5.2% were observed when 1% and 2% of nS, respectively, were added into the P10 mortar (Figure 3b). At the RWP ratio of 15%, the extents of compressive strength rise were lower (2.2 % for P15E2N1, and 3.4% for P15E2N2) . Considering the negative effect of EVA on compressive strength

of cementitious materials [25, 30], the compressive strength increases would come from the microstructure densification by the addition of nS [32, 34].

$$X_{av}(mm) = \frac{X_1 + X_2 + X_3 + X_4 + X_5}{5}$$

Figure 2. Measurements of the average carbonation depth on a cross-section of a split specimen after carbonation.

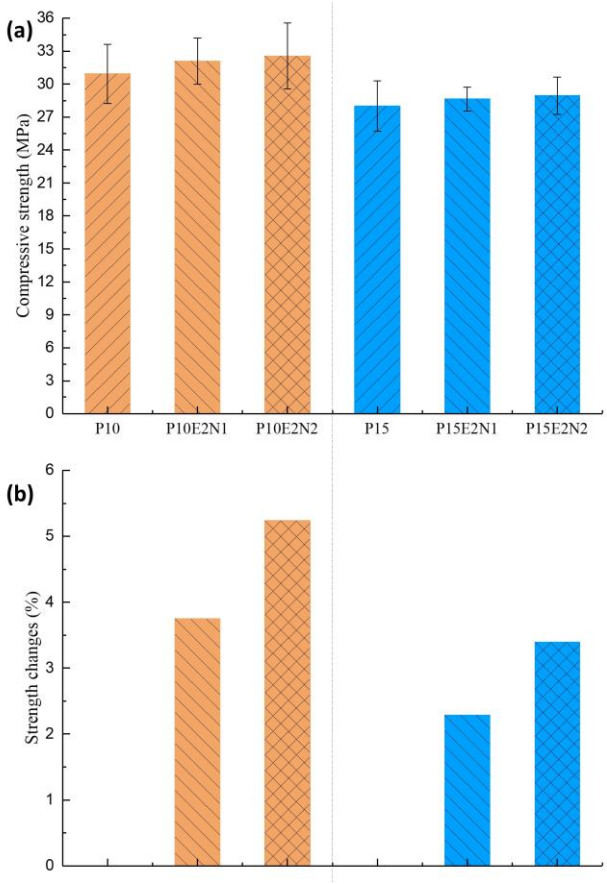

Figure 3. Compressive strength of mortars at 28 d (a) and the relative strength changes (b).

Figure 4a shows the flexural strength for the mortars with 10% and 15% RWP. Like the data of compressive strength, the increase of RWP content from 10% to 15% caused a slight strength drop by roughly 5%, which is due to the increased weak ITZs between RWPs and cement paste compared with that of standard concrete [37]. The combined use of EVA and nS slightly raised the flexural strength by about 2.0% and 1.5% for P10E2N1 and P10E2N2, respectively, when compared with P10 (Figure 4b). For the mortars with 15% RWP, the addition of EVA and nS surprisingly decreased the flexural strength by 0.77% and 1.1% for P15E2N1 and P15E2N2 when compared with P15 (Figure 4b). This means that the effect of mortar compactness on compressive strength may not have the same substantial impact on flexural strength [38]. Similar results have been reported elsewhere [39, 40].

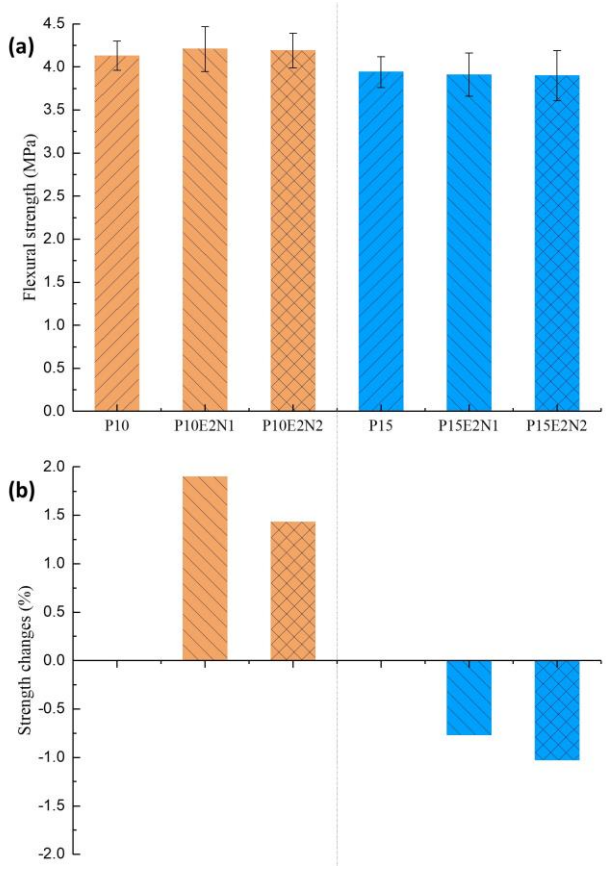

Figure 4. Flexural strength of mortars at 28 d (a) and the relative strength changes (b).

3.2. Carbonation

Immediately after the carbonation test (Figure 2), prisms were split and sprayed with phenolphthalein, where measurements of carbonation depth took place. Figure 5 shows representative cross sections of the tested mortars. In the figure, the white small particles are the RWP aggregates, while the gray and purple red areas represent the carbonated and uncarbonated cement matrix, respectively . The

carbonation depths can be easily distinguished (see the dotted lines in Figure 5).

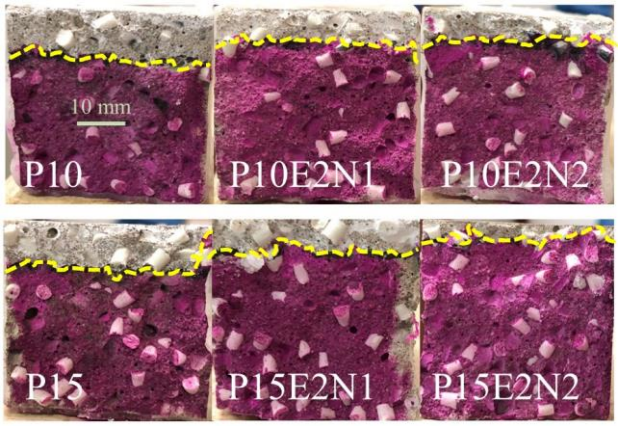

Figure 5. Cross sections of the 28 d mortars after being split and sprayed with phenolphthalein to measure depth of carbonation.

Carbonation depths were measured with an accurate caliper to the nearest 0.01 mm. Figure 6 shows the averaged carbonation depths for all 28 d mortars. The specimens with 15% RWP showed thicker carbonation depth than those with 10% RWP. This may be due to the fact that more RWP aggregate induced more porous aggregate-matrix ITZs that facilitate CO_2 migration. Clearly, the addition of nS greatly reduced the carbonation depths. The use of 2% nS in mortars with 10% and 15% RWPs caused the carbonation depth decreases by around 48% and 47% for P10E2N2 compared to P10 and P15E2N2 compared to P15, respectively. These findings are in line with previous studies [8, 41].

Figure 7 shows SEM images of cement matrix (P10 and P10E2N2 were given as an example) in a carbonated zone. In Figure 7a, typical cement hydration products (AFt/AFm, CSH) can be seen on the left side of the image with a higher magnification subfigure in the bottom left. On the right side, rhombohedral clusters were observed and tested with EDS, which were believed to be carbonated products [42]: aragonite and calcite. The formation of such carbonation products has been verified elsewhere [5, 9, 33, 43]. The average side length of the rhombohedrons was around 8 μm, as measured in the right subfigure. In addition to the hydrated and carbonated products observed in P10 (Figure 7a), P10E2N2 (Figure 7b) shows distinct micro morphology of the polymer EVA films that comes at a cost of less growth of cement hydrated products [29], see the subfigure on the right side with higher magnification. The role of nanosilica as a filler synergistically improved the microstructure of mortars, which in turn improved carbonation resistance [33, 41].

4. Concluding remarks

In this work, carbonation resistance of cement mortars with RWP aggregate were tested. EVA of 2 wt% and nS of 1 and 2 wt% were blended with cement mortars to enhance their carbonation resistance. The following concluding remarks can be drawn:

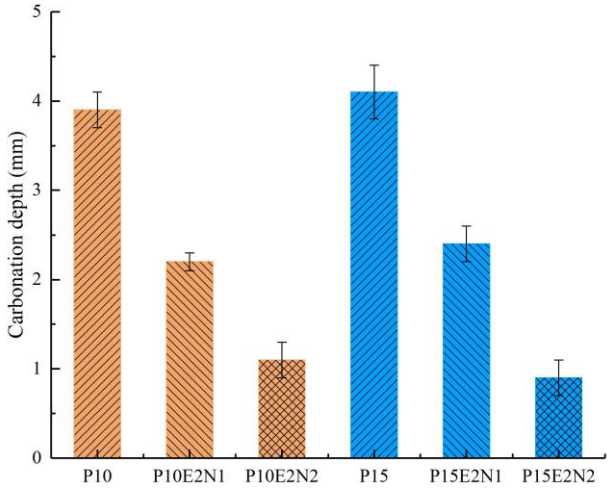

Figure 6. Carbonation depths of the 28 d tested mortars.

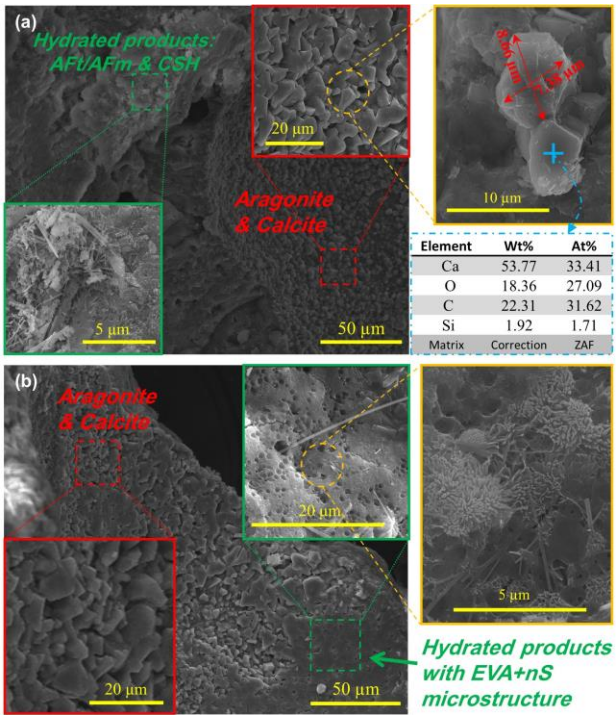

Figure 7. SEM/EDS images and data showing an example of a carbonated zone of the 28-d sample P10 (a) and P10E2N2 (b) after being in the carbonation chamber for 21 days.

- The combined use of EVA and nS increased compressive strength, and the increasing extents for the mortars with 10% RWP were higher than those with 15% RWP.
- Flexural strength was enhanced for the mortars with 10% RWP. The increase of nS content

caused the worse flexural strength for the mortars with 15% RWP.

- Carbonation depths was substantially reduced by ~50% for the mortars with 2% nS. The combined use of EVA and nS provides a promising technique to improve the carbonation resistance of cementitious materials with RWPs.

Acknowledgment

This research is supported by Key Project of NSFC (52038004) and NSFC (51878602).

REFERENCES

1. Cao, Y., et al., 2019. Critical chloride content in reinforced concrete — An updated review considering Chinese experience. Cement and Concrete Research, 117: p. 58-68.
2. Habert, G., et al., 2020. Environmental impacts and decarbonization strategies in the cement and concrete industries. Nature Reviews Earth & Environment, 1(11): p. 559-573.
3. Nguyen, M.H., K. Nakarai, and R. Torrent, 2020. Service life prediction of steam-cured concrete utilizing in-situ air permeability measurements. Cement and Concrete Composites, 114: p. 103747.
4. Chen, T. and X. Gao, 2019. How carbonation curing influences ca leaching of Portland cement paste: Mechanism and mathematical modeling. Journal of the American Ceramic Society, 102(12): p. 7755-7767.
5. Jiang, Y. and T.-C. Ling, 2020. Production of artificial aggregates from steel-making slag: Influences of accelerated carbonation during granulation and/or post-curing. Journal of CO2 Utilization, 36: p. 135-144.
6. Dos Reis, G.S., et al., 2021. Coupling of attrition and accelerated carbonation for CO2 sequestration in recycled concrete aggregates. Cleaner Engineering and Technology, 3: p. 100106.
7. Fang, X., et al., 2021. Fast enhancement of recycled fine aggregates properties by wet carbonation. Journal of Cleaner Production, 313: p. 127867.
8. Li, L., et al., 2021. Efficiencies of carbonation and nano silica treatment methods in enhancing the performance of recycled aggregate concrete. Construction and Building Materials, 308: p. 125080.
9. Yan, D., et al., 2021. CO2 Pretreatment to Aerated Concrete with High-Volume Industry Wastes Enables a Sustainable Precast Concrete Industry. ACS Sustainable Chemistry & Engineering,
10. Mi, R., et al., 2021. Carbonation resistance study and inhomogeneity evolution of recycled aggregate concretes under loading effects. Cement and Concrete Composites, 118: p. 103916.
11. Liu, K., et al., 2021. Prediction of carbonation depth for recycled aggregate concrete using ANN hybridized with swarm intelligence algorithms. Construction and Building Materials, 301: p. 124382.
12. Liu, P., Z. Yu, and Y. Chen, 2020. Carbonation depth model and carbonated acceleration rate of concrete under different environment. Cement and Concrete Composites, 114: p. 103736.
13. Material Economics, 2018: The Circular Economy - a Powerful Force for Climate Mitigation. Sweden.
14. Monteiro, P.J.M., S.A. Miller, and A. Horvath, 2017. Towards sustainable concrete. Nature Materials, 16(7): p. 698-699.
15. Al-Mansour, A., et al., 2022. Sustainable cement mortar with recycled plastics enabled by the matrix-aggregate compatibility improvement. Construction and Building Materials, 318: p. 125994.
16. Shah, S.N., et al., 2021. Lightweight foamed concrete as a promising avenue for incorporating waste materials: A review. Resources, Conservation and Recycling, 164: p. 105103.
17. Adnan, H.M. and A.O. Dawood, 2021. Recycling of plastic box waste in the concrete mixture as a percentage of fine aggregate. Construction and Building Materials, 284: p. 122666.
18. Tayeh, B.A., D.M.A. Saffar, and R. Alyousef, 2020. The Utilization of Recycled Aggregate in High Performance Concrete: A Review. Journal of Materials Research and Technology, 9(4): p. 8469-8481.
19. Olofinnade, O., S. Chandra, and P. Chakraborty, 2020. Recycling of high impact polystyrene and low-density polyethylene plastic wastes in lightweight based concrete for sustainable construction. Materials Today: Proceedings,
20. Yan, K., et al., 2021. Influence of ethylene-vinyl acetate on the performance improvements of low-density polyethylene-modified bitumen. Journal of Cleaner Production, 278: p. 123865.
21. Cotto-Ramos, A., et al., 2020. Experimental design of concrete mixtures using recycled plastic, fly ash, and silica nanoparticles. Construction and Building Materials, 254: p. 119207.
22. Canto, L.B., 2019. Aspects regarding the efficiency of nanosilica as an interfacial compatibilizer of a polypropylene/ethylene vinyl-acetate immiscible blend. Polymer Testing, 73: p. 135-142.
23. Saradhi Babu, D., K. Ganesh Babu, and T.H. Wee, 2005. Properties of lightweight expanded polystyrene aggregate concretes containing fly ash. Cement and Concrete Research, 35(6): p. 1218-1223.
24. Choi, Y.-W., et al., 2005. Effects of waste PET bottles aggregate on the properties of concrete. Cement and Concrete Research, 35(4): p. 776-781.
25. Liang, G., et al., 2021. Synergistic effect of EVA, TEA and C-S-Hs-PCE on the hydration process and mechanical properties of Portland cement paste at early age. Construction and Building Materials, 272: p. 121891.
26. Mikhailenko, P., et al., 2018. Influence of physico-chemical characteristics on the carbonation of cement paste at high replacement rates of

metakaolin. Construction and Building Materials, 158: p. 164-172.
27. Pu, L. and C. 2018. Unluer, Durability of carbonated MgO concrete containing fly ash and ground granulated blast-furnace slag. Construction and Building Materials, 192: p. 403-415.
28. Sigvardsen, N.M., M.R. Geiker, and L.M. Ottosen, 2021. Reaction mechanisms of wood ash for use as a partial cement replacement. Construction and Building Materials, 286: p. 122889.
29. Peng, Y., et al., 2020. In-situ assessment of the water-penetration resistance of polymer modified cement mortars by μ-XCT, SEM and EDS. Cement and Concrete Composites, 114: p. 103821.
30. Li, H., et al., 2021. Influence of defoaming agents on mechanical performances and pore characteristics of Portland cement paste/mortar in presence of EVA dispersible powder. Journal of Building Engineering, 41: p. 102780.
31. Silva, R.V., J. de Brito, and N. Saikia, 2013. Influence of curing conditions on the durability-related performance of concrete made with selected plastic waste aggregates. Cement and Concrete Composites, 35(1): p. 23-31.
32. Sharma, U., et al., 2019. Effect of particle size of nanosilica on microstructure of C-S-H and its impact on mechanical strength. Cement and Concrete Composites, 97: p. 312-321.
33. Lim, S. and P. Mondal, 2015. Effects of incorporating nanosilica on carbonation of cement paste. Journal of Materials Science, 50(10): p. 3531-3540.
34. Li, L.G., et al., 2017. Combined effects of micro-silica and nano-silica on durability of mortar. Construction and Building Materials, 157: p. 337-347.
35. Jack M. Chi, R.H., C. C. Yang, 2002. Effects of Carbonation on Mechanical Properties and Durability of Concrete Using Accelerated Testing Method. Journal of Marine Science and Technology, 10(1).
36. Correia, J.R., J.S. Lima, and J. de Brito, 2014. Post-fire mechanical performance of concrete made with selected plastic waste aggregates. Cement and Concrete Composites, 53: p. 187-199.
37. Gu, L. and T. Ozbakkaloglu, 2016. Use of recycled plastics in concrete: A critical review. Waste Management, 51: p. 19-42.
38. Sikora, P., et al., 2020. Evaluating the effects of nanosilica on the material properties of lightweight and ultra-lightweight concrete using image-based approaches. Construction and Building Materials, 264: p. 120241.
39. Kancharla, R., et al., 2021. Flexural Behavior Performance of Reinforced Concrete Slabs Mixed with Nano- and Microsilica. Journal of Nanomaterials, 2021: p. 1754325.
40. Sikora, P., et al., 2015. The Effect of Nanosilica on the Mechanical Properties of polymer-Cement Composites (PCC). Procedia Engineering, 108: p. 139-145.
41. Li, L.G., et al., 2021. Synergistic cementing efficiencies of nano-silica and micro-silica in carbonation resistance and sorptivity of concrete. Journal of Building Engineering, 33: p. 101862.
42. Santos, R.M., P. Ceulemans, and T. Van Gerven, 2012. Synthesis of pure aragonite by sonochemical mineral carbonation. Chemical Engineering Research and Design, 90(6): p. 715-725.
43. Morandeau, A., M. Thiéry, and P. Dangla, 2014. Investigation of the carbonation mechanism of CH and C-S-H in terms of kinetics, microstructure changes and moisture properties. Cement and Concrete Research, 56: p. 153-170.